

## ASCA DETECTION OF PULSED X-RAY EMISSION FROM PSR J0631+1036

KEN'ICHI TORII,<sup>1</sup> Y. SAITO,<sup>2</sup> F. NAGASE,<sup>2</sup> T. YAMAGAMI,<sup>2</sup> T. KAMAE,<sup>3</sup> M. HIRAYAMA,<sup>4</sup> N. KAWAI,<sup>1,5,6</sup>  
I. SAKURAI,<sup>1</sup> M. NAMIKI,<sup>1</sup> S. SHIBATA,<sup>7</sup> S. GUNJI,<sup>7</sup> AND J. P. FINLEY<sup>8</sup>

Received 2000 July 27; accepted 2001 March 16; published 2001 April 12

### ABSTRACT

ASCA's long look at the 288 ms radio pulsar PSR J0631+1036 reveals coherent X-ray pulsation from this source for the first time. The source was first detected in a serendipitous *Einstein* observation and later identified as a radio pulsar. Possible pulsation in the  $\gamma$ -ray band has been detected in the *Compton Gamma Ray Observatory* EGRET data. The X-ray spectrum in the ASCA band is characterized by a hard power-law-type emission with a photon index of  $\approx 2.3$ , when fitted with a single power-law function modified with absorption. An additional blackbody component of  $kT \approx 0.14$  keV increases the quality of the spectral fit. The observed X-ray flux is  $2.1 \times 10^{-13}$  ergs s<sup>-1</sup> cm<sup>-2</sup> in the 1–10 keV band. We find that many characteristics of PSR J0631+1036 are similar to those of middle-aged  $\gamma$ -ray pulsars such as PSR B1055–52, PSR B0633+17 (Geminga), and PSR B0656+14.

*Subject headings:* pulsars: general — pulsars: individual (PSR J0631+1036) — stars: neutron — X-rays: stars

### 1. INTRODUCTION

Studies of rotation-powered pulsars in the X-ray band give us information about the evolution of their magnetospheric activities, about their surface temperatures, and about the interaction of the pulsar wind with the surrounding medium (e.g., Becker & Trümper 1997; Saito 1998). The most energetic Crab-like pulsars with spin-down powers of  $\dot{E} \geq 10^{37}$  ergs s<sup>-1</sup> show X-ray pulsations of magnetospheric origin. Most of them are associated with a supernova remnant and power synchrotron nebulae as a result of the shock interaction of the pulsar wind with the ambient medium. The Vela-like pulsars, characterized by their spin-down powers of  $10^{36}$  ergs s<sup>-1</sup>  $\leq \dot{E} \leq 10^{37}$  ergs s<sup>-1</sup>, are embedded in the extended synchrotron nebulae; this often makes it difficult to study the neutron star itself. Older and weaker ( $10^{34}$  ergs s<sup>-1</sup>  $\leq \dot{E} \leq 10^{35}$  ergs s<sup>-1</sup>) sources show pulsating blackbody-type spectra below  $\approx 0.5$ – $0.6$  keV as well as pulsating power-law-type spectra in the hard-energy band. Typical objects of this class are the Three Musketeers, PSR B1055–52, PSR B0656+14, and PSR B0633+17 (Geminga; e.g., Finley, Ögelman, & Kiziloğlu 1992; Greiveldinger et al. 1996; Becker et al. 1999). Interestingly, these middle-aged ( $\tau \approx 10^5$ – $10^6$  yr) pulsars convert their spin-down power into high-energy  $\gamma$ -ray photons with higher efficiencies than is seen in younger pulsars (e.g., Thompson 1996; Kifune 1996).

The source studied herein, PSR J0631+1036, was discovered by the targeted searches for radio pulsars in unidentified *Einstein* X-ray sources (Zepka et al. 1996). The pulse period,

$P \approx 0.288$  s, and its derivative,  $\dot{P} \approx 1.0 \times 10^{-13}$  s s<sup>-1</sup>, give a characteristic age of  $\tau = P/(2\dot{P}) = 4.3 \times 10^4$  yr. The spin-down power is  $\dot{E} = 5.4 \times 10^{34} I_{45}$  ergs s<sup>-1</sup>, where  $I_{45}$  is the moment of inertia of the neutron star normalized to  $10^{45}$  g cm<sup>2</sup>. This range of parameters is between the Vela-like pulsars and the Three Musketeers.

In the *Einstein* IPC data, about 50 photons were detected from the X-ray counterpart of the radio pulsar PSR J0631+1036. The spectral fit gave a blackbody temperature of  $kT = 0.27 \pm 0.08$  keV, an absorption column of  $N_{\text{H}} = (9 \pm 4) \times 10^{21}$  cm<sup>-2</sup>, and an observed X-ray flux of  $F_{\text{X}} = 1.9 \times 10^{-13}$  ergs s<sup>-1</sup> cm<sup>-2</sup> in the 0.16–3.5 keV band (Zepka et al. 1996). Unfortunately, the source was located on the support rib of the IPC field. This made the source position and source spectra rather uncertain. Later, the source was serendipitously observed in the field of view of the *ROSAT* Position Sensitive Proportional Counter (PSPC). Spectral analysis gave a best-fit blackbody temperature of  $kT = 0.18 \pm 0.08$  keV, an absorption column of  $N_{\text{H}} = (1.2 \pm 0.6) \times 10^{21}$  cm<sup>-2</sup>, and an effective radius of the emitting region of approximately  $R_{\text{BB}} \approx 1$  km (Zepka et al. 1996). Again, the source was unfortunately shadowed by the detector-supporting ribs, making the obtained spectral parameters rather uncertain.

Interestingly, it was found that this source might be pulsating in the  $\gamma$ -ray energy band. Zepka et al. (1996) folded the arrival times of 267 counts from the *Compton Gamma Ray Observatory* EGRET at the expected pulse period. They found that the folded light curve was significantly displaced from uniform distribution at more than 99% confidence.

### 2. OBSERVATION

We have proposed and carried out the ASCA observation of PSR J0631+1036 during 1998 October 16–18. ASCA (Tanaka, Inoue, & Holt 1994) carries two kinds of X-ray detectors at the foci of four identical X-ray telescopes. The X-ray CCD camera (the Solid-State Imaging Spectrometer [SIS]; Burke et al. 1994) has the higher energy resolution and a relatively high detection efficiency in the soft-energy band. The time resolution of SIS is 4–16 s in the standard mode, which is not suitable for timing observations of fast pulsars. The imaging gas-scintillation proportional counter (the Gas Imaging Spectrometer [GIS]; Ohashi et al. 1996; Makishima et al. 1996) has a relatively high detection

<sup>1</sup> Cosmic Radiation Laboratory, Institute of Physical and Chemical Research (RIKEN), Wako, Saitama, 351-0198, Japan; torii@crab.riken.go.jp.

<sup>2</sup> Institute of Space and Astronautical Science, 3-1-1, Yoshinodai, Sagami-cho, Kanagawa, 229-8510, Japan; saito@balloon.isas.ac.jp.

<sup>3</sup> Graduate School of Science, Hiroshima University, 1-3-1, Kagamiyama, Higashihiroshima, 739-8526, Japan.

<sup>4</sup> Santa Cruz Institute for Particle Physics, University of California at Santa Cruz, Santa Cruz, CA 95064.

<sup>5</sup> Space Utilization Research Program, Tsukuba Space Center, National Space Development Agency of Japan, 2-1-1, Sengen, Tsukuba, Ibaraki, 305-8505, Japan.

<sup>6</sup> Department of Physics, Tokyo Institute of Technology, 2-12-1, Ookayama, Meguro-ku, Tokyo, 152-8551, Japan.

<sup>7</sup> Department of Physics, Yamagata University, 1-4-12, Kojirakawa, Yamagata, 990-8560, Japan.

<sup>8</sup> Department of Physics, Purdue University, West Lafayette, IN 47907.

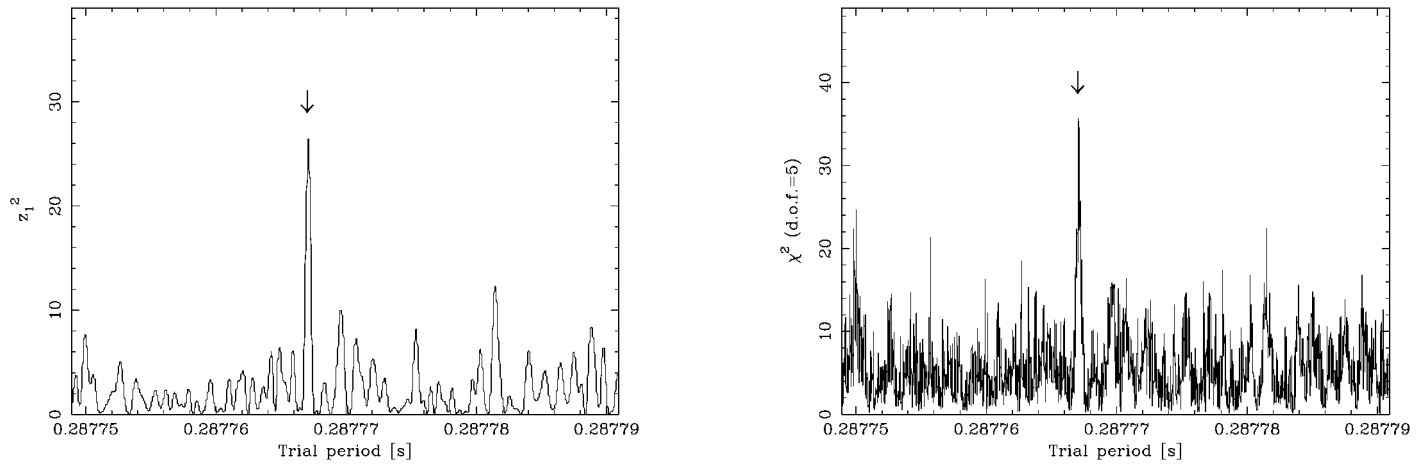


Fig. 1.—The  $z_1^2$  and  $\chi^2$  plotted as a function of trial periods. The arrows show the expected period from the effective radio ephemeris.

efficiency in the hard-energy band and high time resolution. We operated the SIS in 1-CCD faint mode with a 4 s time resolution. Therefore, only pulse-phase-averaged spectroscopy could be made with the SIS. We operated the GIS in the PH mode and assigned a part of the telemetry bit to increase the time resolution reducing the spectral information. The resultant time resolution was 3.9 ms or better depending on the telemetry rate. We used screened event data according to the standard REV2 processing.<sup>9</sup> The effective exposure time was 69.6 and 76.1 ks for SIS and GIS, respectively, and the net time span of the observation was  $T = 160$  ks.

### 3. ANALYSIS

#### 3.1. Timing

We analyzed the GIS data in order to search for pulsations in the X-ray band. The GIS observation began at MJD 51,103.0185 and ended at MJD 51,104.8260. The data from GIS2 and GIS3 were co-added, yielding  $\approx 1100$  events within a  $3'$  radius circular region for a total energy band of 0.7–7 keV, including background. The photon arrival times were barycentered, and a  $z_1^2$  test (Buccheri et al. 1983) and an epoch-folding search (e.g., Leahy et al. 1983) were applied, bracketing the expected period,  $P_{\text{exp}} = 0.2877671$  s at MJD 51,103.9305 (the middle time of the current ASCA observation at barycenter), from the radio ephemeris that was effective during the current observation (D. Nice 2000, private communication).

The left panel of Figure 1 shows the result of the  $z_1^2$  test. We can clearly see a peak at the expected pulse period. No similar peaks have been found in the background data with better statistics extracted from the same observation. We then applied the epoch-folding search. The events were folded into 6 bins, and  $\chi^2$ -values were calculated from each trial period. A significant peak is found (Fig. 1, right panel) at the period consistent with that obtained from the  $z_1^2$  test. The probabilities of finding higher peaks out of random fluctuations with a single trial are as low as  $1.8 \times 10^{-6}$  for the  $z_1^2$  test and as low as  $1.1 \times 10^{-6}$  for the folding search. Considering the reasonable number of independent trials ( $\approx 18$ ) as discussed below, the chance probabilities of finding higher peaks are  $3.2 \times 10^{-5}$  for the  $z_1^2$  test and  $2.0 \times 10^{-5}$  for the folding search. Therefore,

we conclude that we have significantly detected X-ray pulsations from PSR J0631+1036 for the first time.

From folding search, the pulse period is determined to be  $P = 0.2877672(1)$  s at MJD 51,103.9305. Here the value in parentheses is a 90% confidence error to the last digit. We estimated this error by using the method of Leahy (1987), which gave tighter constraint than the nominal error of  $P^2/(2T) = 3 \times 10^{-7}$  s.

The detected pulse period is consistent with the effective radio ephemeris, while it is significantly shorter than the period  $P = 0.2877676$  s that was extrapolated from the previous radio ephemeris (Zepka et al. 1996) by  $\Delta P = -4 \times 10^{-7}$  s. This difference in period may not be ascribed to a finite value of negative  $\dot{P}$  since the corresponding value of  $\dot{P} \approx -3 \times 10^{-23}$  s $^{-1}$  gives an unreasonably large braking index,  $n \approx 7 \times 10^2$ . Although it is not known whether or not PSR J0631+1036 has recently had a glitch because of a lack of published results (e.g., Johnston & Galloway 1999), we consider that the value of  $\Delta P/P = -1.4 \times 10^{-6}$  is naturally interpreted as the result of glitch activity. The reasonable number of independent trials for the current timing analysis is then estimated by considering a large glitch of  $|\Delta P/P| \lesssim 10^{-5}$  during the 4.3 yr between the last published radio observation (Zepka et al. 1996) and the ASCA observation. The largest glitch ever observed would fall within the range considered here (Wang et al. 2000). Then the number of independent Fourier bins covering the period range  $P_{\text{exp}} - |\Delta P_{\text{exp}}| < P < P_{\text{exp}} + |\Delta P_{\text{exp}}|$  would be 18.

The top panel of Figure 2 shows the folded light curves in the total energy band. The pulse shape is singly peaked and sinusoidal. The pulse amplitude is  $45\% \pm 16\%$  of the source flux, excluding background. A comparison has been made of pulse profiles in different energy bands. The pulse amplitudes, derived by fitting the profiles with a sinusoidal curve, are  $31_{-17}^{+12}\%$  and  $63\% \pm 18\%$  in the 0.7–1.9 and 1.9–7 keV bands, respectively.

#### 3.2. Spectrum

We analyzed the pulse-phase-averaged spectra by using both the SIS and GIS data. Spectra were extracted from circular regions of  $3'$  radius. Background was subtracted from the same observation. For the SIS, events from the whole chip, excluding the circular region of  $4'$  radius around the source, were used as background. For the GIS, events from circular regions of

<sup>9</sup> See E. A. Pier's 1997 ASCA getting started guide for revision 2 data, version 6.1 (available at <ftp://legacy.gsfc.nasa.gov/asca/doc>).

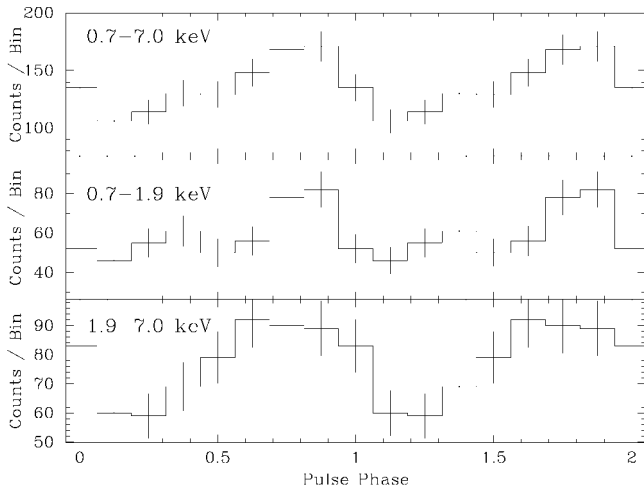


FIG. 2.—Folded pulse profiles shown for the full energy range of 0.7–7.0 keV (*top panel*) and for two subranges of 0.7–1.9 keV (*middle panel*) and 1.9–7.0 keV (*bottom panel*). The vertical axes show the number of events in each bin, and they are displayed so that the background levels correspond to the baseline of each panel. Two complete cycles are plotted for clarity.

7/5 radius to the northeast of the source were used as background.

A single power-law function with soft X-ray absorption was first applied to the spectrum from each detector. This simple model gave an acceptable fit to each data set, and the spectral parameters were found to be consistent with each other within statistical errors. Therefore, we simultaneously fitted the two SIS and two GIS spectra. In the fitting procedure, each data point was weighted according to the statistics (the number of photons in each bin), taking into account the propagation of error due to background subtraction. For clarity, Figure 3 shows the representative spectra and the best-fit model function for the two detectors (SIS1 and GIS3). The best-fit parameters are the power-law photon index  $\gamma = 2.3^{+0.5}_{-0.4}$ , the absorbing hydrogen column density  $N_{\text{H}} = 0.2^{+0.2}_{-0.1} \times 10^{22} \text{ cm}^{-2}$ , and the normalization  $7_{-2}^{+3} \times 10^{-5} \text{ photons keV}^{-1} \text{ s}^{-1} \text{ cm}^{-2}$  at 1 keV with  $\chi^2/\text{degrees of freedom (dof)} = 140.6/112$ . These errors are at one-parameter 90% confidence. The observed flux is  $f_{\text{X}} = 1.9 \times 10^{-13} \text{ ergs s}^{-1} \text{ cm}^{-2}$  and the intrinsic flux is  $f_{\text{X}} = 2.0 \times 10^{-13} \text{ ergs s}^{-1} \text{ cm}^{-2}$ , corresponding to a luminosity of  $L_{\text{X}} = 2.4 \times 10^{31} d_1^2 \Omega_{4\pi} \text{ ergs s}^{-1}$ , all in the 1–10 keV range. Here  $d_1$  is the source distance normalized to 1 kpc, and  $\Omega_{4\pi}$  is the emitting solid angle normalized to  $4\pi$  steradian. A single blackbody model with absorption gave a best-fit temperature of  $kT = 0.43 \text{ keV}$ , while the fit was not acceptable with  $\chi^2/\text{dof} = 178.9/112$ .

Since the soft X-ray emission was well fitted by a blackbody model (Zepka et al. 1996), we tried a blackbody plus power-law model, modified by a single absorption component. When the blackbody temperature and the normalization were fixed at the best-fit parameters derived from the *ROSAT* PSPC,  $kT = 0.18 \text{ keV}$  and  $R_{\text{BB}} = 1 \text{ km}$  at 1 kpc, the following parameters were obtained. The power-law photon index  $\gamma = 1.2 \pm 0.4$ , the normalization for the power-law component  $\text{norm.} = 2.1^{+1.4}_{-0.9} \times 10^{-5} \text{ photons keV}^{-1} \text{ s}^{-1} \text{ cm}^{-2}$  at 1 keV, and the absorption column  $N_{\text{H}} = 0.96^{+0.08}_{-0.07} \times 10^{22} \text{ cm}^{-2}$ . In this case, the crossover of the two components occurs at around 1.9 keV. The quality of the fit is slightly worse than the single power-law model,  $\chi^2/\text{dof} = 147.1/112$ . When the emitting radius of the blackbody is set free,  $R_{\text{BB}} = (0.6^{+0.1}_{-0.2}) d_1 \text{ km}$  is obtained with

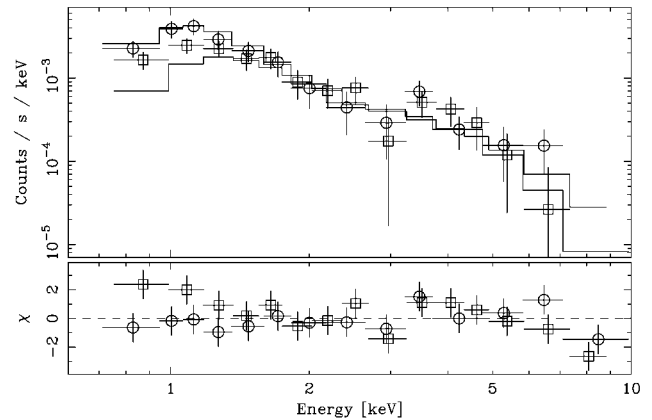


FIG. 3.—*Top panel*: Observed energy spectra and best-fit absorbed power-law function shown for the two representative detectors. *Bottom panel*: Residuals normalized by the standard deviations. The circles and squares show SIS1 and GIS3 data, respectively.

$\gamma = 1.7 \pm 0.4$ ,  $\text{norm.} = 4_{-1}^{+2} \times 10^{-5} \text{ photons keV}^{-1} \text{ s}^{-1} \text{ cm}^{-2}$ ,  $N_{\text{H}} = (0.5 \pm 0.2) \times 10^{22} \text{ cm}^{-2}$ , and  $\chi^2/\text{dof} = 128.2/111$ .

Starting with the best-fit parameters for the blackbody component obtained from *ROSAT*, we tried to set all the five parameters free in the two-component (blackbody plus power-law) model. However, the parameters could not be well constrained because of trade-offs between the two continuum components and the arbitrary absorption column. Therefore, we fixed the temperature at a value in the range of  $0.1 \text{ keV} \leq kT \leq 0.3 \text{ keV}$  with every 0.01 keV step. Then the minimum of  $\chi^2/\text{dof} = 126.1/111$  was obtained with  $kT = 0.14 \text{ keV}$  and  $R_{\text{BB}} = (2.1^{+0.5}_{-0.6}) d_1 \text{ km}$ . The  $\chi^2$ -value with  $kT = 0.14 \text{ keV}$  is thus smallest, and we consider this model to be the most suitable for the current *ASCA* data. The other spectral parameters for  $kT = 0.14 \text{ keV}$  are the power-law photon index  $\gamma = 1.9 \pm 0.4$ , the normalization for the power-law component  $6_{-2}^{+3} \times 10^{-5} \text{ photons keV}^{-1} \text{ s}^{-1} \text{ cm}^{-2}$  at 1 keV, and the absorption column  $N_{\text{H}} = (0.8 \pm 0.2) \times 10^{22} \text{ cm}^{-2}$ . With this model, the total observed X-ray flux is  $f_{\text{X}} = 2.1 \times 10^{-13} \text{ ergs s}^{-1} \text{ cm}^{-2}$ , and the intrinsic flux is  $f_{\text{X}} = 3.5 \times 10^{-13} \text{ ergs s}^{-1} \text{ cm}^{-2}$  in the 1–10 keV band. The corresponding luminosity is  $4.2 \times 10^{31} d_1^2 \Omega_{4\pi} \text{ ergs s}^{-1}$ . The blackbody component contributes 16% of the observed flux and 34% of the intrinsic flux.

We then examined the pulse-phase dependence of the spectral shape by using the GIS data. We divided the data into two subsets, the pulse-on (high-intensity) phase and the pulse-off (low-intensity) phase. The two phases are split at phase 0.0625 and phase 0.5625, respectively, in Figure 2. Since the statistics are limited, we fixed the absorption column at the best-fit value obtained from a single power-law model and fitted the spectra with a single power-law function. The photon indices were  $\gamma = 2.5^{+0.7}_{-0.5}$  and  $\gamma = 3.5^{+1.0}_{-0.9}$  for the pulse-on and pulse-off phases, respectively. Although a harder spectrum is suggested for a higher flux phase, the photon indices are consistent within statistical errors.

#### 4. DISCUSSION

The overall properties of the multiwavelength spectrum of PSR J0631+1036 from radio to X-ray and  $\gamma$ -ray are similar to those of other  $\gamma$ -ray pulsars (Thompson 1996). They are radiating a large fraction ( $\geq 0.1$ ) of their spin-down power in the  $\gamma$ -ray band. The X-ray luminosity  $L_{\text{X}} = 4.2 \times 10^{31} d_1^2 \Omega_{4\pi} \text{ ergs s}^{-1}$  obtained from the two-component spectral fit is

$\approx 0.08 d_1^2 \Omega_{4\pi} I_{45}^{-1}$ % of the spin-down power, which is comparable to those of the Vela pulsar and the Three Musketeers (e.g., Saito 1998). For PSR J0631+1036, the power-law photon index that smoothly connects the X-ray flux and the  $\gamma$ -ray flux is  $\gamma \approx 1.2$ . Therefore, the simple extension of the X-ray spectrum with a photon index of  $\gamma = 1.9 \pm 0.4$ , obtained from the best power-law plus blackbody model, predicts lower  $\gamma$ -ray flux than observed. This situation may be reconciled with complete pulse-phase spectroscopy, including an appropriate blackbody model, which should be done in future observations.

The observed pulse fraction, which is 45% in the 0.7–7 keV band, is comparable to the  $\approx 40\%$  found for PSR B1055–52 above 1 keV (Ögelman & Finley 1993; also see Fig. 1, *right panel*) and the  $\approx 55\%$  found for Geminga in the 1–4 keV band (Halpern & Wang 1997). These values are significantly larger than the pulse fraction of  $14\% \pm 2\%$  for PSR B0656+14 as measured by *ROSAT* (Finley et al. 1992). This might partly be due to the energy-dependent pulse fraction of PSR B0656+14.

The significant difference between the detected and extrapolated pulse periods may be understood as a result of glitch activity. Urama & Okeke (1999) have found that there exists a good correlation between young pulsars' spin-down rates and glitch activity. They predict the interval between Vela-size glitches of average  $\Delta P/P = -2 \times 10^{-6}$  to be 7 yr for PSR J0631+1036. In terms of the glitch-activity parameter  $A_g$ , which is the mean fractional change in period per year owing to glitches, the predicted value is  $A_g = 3.09 \times 10^{-7} \text{ yr}^{-1}$  (Urama & Okeke 1999). This corresponds to an accumulated period change during 4.3 yr of  $\Sigma(\Delta P/P) \approx -1.3 \times 10^{-6}$ . These predictions are in good agreement with those observed,  $A_g = 3.2 \times 10^{-7} \text{ yr}^{-1}$  or  $\Sigma(\Delta P/P) = -1.4 \times 10^{-6}$ .

On the other hand, Lyne, Shemar, & Graham-Smith (2000) studied the statistical properties of pulsar glitches by using well-defined samples and found a strong indication that pulsars with large magnetic fields suffer many small glitches while others show a smaller number of large glitches. Comparing the period

and its derivative for PSR J0631+1036 with those in their sample, we find that PSR B1758–23, possibly associated with the supernova remnant W28 (Kaspi et al. 1993), has a similar range of parameters. Therefore, PSR J0631+1036 might have experienced a large number of medium-size ( $\Delta P/P \approx -10^{-7}$ ) glitches, as in the case of PSR B1758–23. Lyne et al. (2000) also found a good correlation between  $\dot{\nu}$  and the glitch spin-up rate,  $\dot{\nu}_{\text{glitch}}$ , defined as the cumulative effect of a glitch on the frequency derivative. The relation  $\dot{\nu}_{\text{glitch}} = -0.017\dot{\nu}$  leads to  $\Delta P = -2.4 \times 10^{-7} \text{ s}$  for PSR J0631+1036 during a time span of 4.3 yr, in reasonable agreement with that observed,  $\Delta P = -4 \times 10^{-7} \text{ s}$ .

PSR J0631+1036 was first detected in the soft X-ray band since it is in the direction of the Galactic anticenter ( $l, b$ ) = (201:22, 0:45), where the interstellar absorption is much smaller than in the Galactic plane toward the Galactic center. Also, the detection of pulsed X-ray emission could only be made with the long-exposure time as performed with *ASCA* and by referring to the previously known radio period. This lesson suggests that there may be other similar sources hidden in the Galactic plane. Combined analyses of radio, X-ray, and unidentified  $\gamma$ -ray sources may be useful (e.g., Roberts, Romani, & Kawai 2001).

In summary, we have detected the pulsed X-ray emission from PSR J0631+1036 for the first time. The negative offset of the observed period from the extrapolated radio ephemeris is attributable to the accumulated change in period due to glitch activity. The X-ray spectrum is well described by a power-law plus blackbody model with an observed flux of  $f_x = 2.1 \times 10^{-13} \text{ ergs s}^{-1} \text{ cm}^{-2}$  in the 1–10 keV band.

The authors thank David Nice for providing us with the radio ephemeris of PSR J0631+1036 prior to publication. The authors are grateful to all the members of the *ASCA* team for making the observation possible.

#### REFERENCES

- Becker, W., Kawai, N., Brinkmann, W., & Mignani, R. 1999, *A&A*, 352, 532  
 Becker, W., & Trümper, J. 1997, *A&A*, 326, 682  
 Buccheri, R., et al. 1983, *A&A*, 128, 245  
 Burke, B. E., Mountain, R. W., Daniels, P. J., Cooper, M. J., & Dolat, V. S. 1994, *IEEE Trans. Nucl. Sci.*, NS-41, 375  
 Finley, J. P., Ögelman, H., & Kiziloğlu, Ü. 1992, *ApJ*, 394, L21  
 Greiveldinger, C., et al. 1996, *ApJ*, 465, L35  
 Halpern, J. P., & Wang, F. Y.-H. 1997, *ApJ*, 477, 905  
 Johnston, S., & Galloway, D. 1999, *MNRAS*, 306, L50  
 Kaspi, V. M., Lyne, A. G., Manchester, R. N., Johnston, S., D'Amico, N., & Shemar, S. L. 1993, *ApJ*, 409, L57  
 Kifune, T. 1996, in *IAU Colloq. 160, Pulsars: Problems and Progress*, ed. S. Johnston, M. A. Walker, & M. Bailes (ASP Conf. Ser. 105; San Francisco: ASP), 339  
 Leahy, D. A. 1987, *A&A*, 180, 275  
 Leahy, D. A., Darbro, W., Elsner, R. F., Weisskopf, M. C., Kahn, S., Sutherland, P. G., & Grindlay, J. E. 1983, *ApJ*, 266, 160  
 Lyne, A. G., Shemar, S. L., & Graham-Smith, F. 2000, *MNRAS*, 315, 534  
 Makishima K., et al. 1996, *PASJ*, 48, 171  
 Ögelman, H., & Finley, J. P. 1993, *ApJ*, 413, L31  
 Ohashi, T., et al. 1996, *PASJ*, 48, 157  
 Roberts, M. S. E., Romani, R. W., & Kawai, N. 2001, *ApJS*, 133, 451  
 Saito, Y. 1998, Ph.D. thesis, Univ. Tokyo (ISAS Res. Note 643)  
 Tanaka, Y., Inoue, H., & Holt, S. S. 1994, *PASJ*, 46, L37  
 Thompson, D. J. 1996, in *IAU Colloq. 160, Pulsars: Problems and Progress*, ed. S. Johnston, M. A. Walker, & M. Bailes (ASP Conf. Ser. 105; San Francisco: ASP), 307  
 Urama, J. O., & Okeke, P. N. 1999, *MNRAS*, 310, 313  
 Wang, N., Manchester, R. N., Pace, R. T., Bailes, M., Kaspi, V. M., Stappers, B. W., & Lyne, A. G. 2000, *MNRAS*, 317, 843  
 Zepka, A., Cordes, J. M., Wasserman, I., & Lundgren, S. C. 1996, *ApJ*, 456, 305